JMEPEG (2014) 23:4289–4297
DOI: 10.1007/s11665-014-1217-z

1059-9495/$19.00

Energy Absorption in a Shear-Thickening Fluid

Seyed Hossein Amiri Afeshejani, Seyed Ali Reza Sabet, Mohammad Ebrahim Zeynali, and Mohammad Atai

(Submitted February 7, 2014; in revised form August 15, 2014; published online September 9, 2014)

This study investigates energy absorption in a shear-thickening fluid (STF) containing nano-size fumed silica as a suspending material. Fumed silica particles in 20, 30, and 40 wt.% were used in polyethylene glycol and ethylene glycol. Three areas were studied, namely: energy absorption of STF pre-impregnated aramid fabric, neat STF under high-velocity impact, and flexible foam soaked in STF under low-velocity drop weight impact. Results showed moderate energy absorption in STF pre-impregnated aramid fabric compared to dry fabric. High-velocity impact tests also revealed higher fabric weave density, and multi-layered target plays vital role in optimum performance of SFT impregnated targets. High-velocity impact tests on the neat STF showed good energy absorption at velocities near STF critical shear rate. Low-velocity drop weight impact test on flexible foam soaked in STF also indicated significant energy absorption.

Keywords composites, materials by design, nanomaterials, organic matrix, polymers and plastics

1. Introduction

Suspensions of non-aggregating solid particles in high concentration if measured in the appropriate shear rate range will always show (reversible) shear-thickening behavior. It is important to note that in suspensions, the shear thickening is almost immediately reversible, that is to say, as soon as the shear rate is decreased, the viscosity (however, high it might be) immediately decreases (Ref 1).

Engineering community initially believed that there is no useful application for dilatancy and that many consider that it offers no positive advantages in industrial situations (Ref 2). One novel application which has emerged in the past two decades has been the utilization of shear-thickening fluid hereafter referred to STF materials for ballistic protection and energy absorption (Ref 3). Ballistic protection materials such as Kevlar®, Twaron®, and Spectra® has been extensively used in various forms; the main reason for their use is their high strength, high tenacity, and lightweight characteristics. With increase in lethality of ballistic threats, efforts were mainly focused on adding more layers and also ceramic insert incorporation with of course increased weight penalty for the armor and reduced mobility of the user. The effectiveness of fabric armor depends on several factors (Ref 4). These factors highlighted by Cheeseman and Bogetti (Ref 5) are material properties of the yarns, fabric weave architecture, projectile geometry, interaction between individual fabric layers, far field boundary conditions, and inter-yarn and fabric-projectile friction. Inter-yarn and fabric-projectile friction plays a significant role in the ballistic performance of the fabric and has been subject of study of numerous researchers. Briscoe and Motamedi (Ref 6, 7), Lavielle et al. (Ref 8), Lee et al. (Ref 9) and as recent as 2008, the subject of the role of projectile's friction during high-velocity impact has been studied by the author and his co-workers (Ref 10). The latter work looked at FRP plates containing different percentages of sand filler in two extreme sizes of sand (75 and 600 μm) under high-velocity impact using sharp nose projectile. STF materials have also been the focus of attention for ballistic protection as a friction enhancing material. Lee et al. (Ref 11) used Kevlar fabric impregnated with a colloidal STF, consisting of silica particles in ethylene glycol. Targets of size 47.6 mm were impregnated with 2, 4, and 8 ml of STF per layer of fabric. They used fragment simulation projectile at high-velocity impact (244 m/s), and reported four layers of Kevlar impregnated STF have nearly the same weight and ballistic performance as 10 layers of un-impregnated layers of same reinforcement. The enhancement provided by the STF was suspected to be the increase in frictional interaction between the yarns. Decker et al. (Ref 12) investigated Stab resistance of STF treated of Kevlar and Nylon fabrics and reported significant improvements over neat fabric targets of equivalent areal density. Improvements in puncture resistance (spike threat) under high- and low-speed loading conditions with a slight increase in cut protection (knife threat) were also part of their findings. Wagner and Brady (Ref 13) reviewed lubrication hydrodynamics and hydroclusters as well as various applications associated with colloidal STF. Rosen et al. (Ref 14) studied the shear thickening of highly loaded kaolin clay suspensions for use in protective Kevlar fabrics and reported a marked increase in spike and needle resistance and a reduction in yarn pullout. The work also reported quasi-static stab tests on four layers of Kevlar impregnated with the kaolin STF, preventing penetration of an NIJ standard spike at loads up to 160 N. The same four layers of neat Kevlar were penetrated at just 35 N. On the issue of strain rate assessment, Lim et al. (Ref 15) studied the transient response of a STF using the split Hopkinson pressure bar technique. Their work involved studying the effect of loading rate on this transition time for particle volume fraction of 0.54 silica suspension. Their result showed that the time required for the transition to occur

Seyed Hossein Amiri Afeshejani, Seyed Ali Reza Sabet, Mohammad Ebrahim Zeynali, and **Mohammad Atai**, Iran Polymer and Petrochemical Institute, P.O. Box 14965/115, Tehran, Islamic Republic of Iran. Contact e-mail: a.sabet@ippi.ac.ir.

Table 1 Properties of Twaron reinforcement

Code	Type	Total areal density, g/m^2	Thickness, mm	Breaking Strength ($N/5_{CM} \times 1000$) Warp/Weft(a)	Fabric areal weight, g, 15 × 25 cm Dry one layer	Fabric areal weight, g, 15 × 25 cm with STF one layer	Added-on STF, %
T717	Plain fabric	280	0.40	92/97	10.5 (0.43)(b)	16.05 (0.40)(b)	53
CT 706	Plain woven roving	215	0.31	10.5/11.1	8.06 (0.65)(b)	12.73 (0.51)(b)	56

(a) Data taken from ballistic material HBK (Ref 27)
(b) Standard deviation on average of three samples measured

decreases logarithmically with loading rate and concluded that the transition is not triggered by a characteristic shear rate, but rather a critical shear strain is required. Hassan et al. (Ref 16) investigated the synthesis and fabrication of STF/fabric composite. They used Kevlar and Nylon fabrics in STF/ethanol solution and Knife threats, and quasi-static penetration tests were performed. They reported that STF impregnated fabrics have better penetration resistance compared to neat fabric without affecting its flexibility. Lee and Kim (Ref 17) looked into reasons for energy absorption enhancement in STF-coated Kevlar fabric; they attributed this enhancement to increase in frictional interaction between yarns in the impregnated fabrics. Majumdar et al. (Ref 18-21) in a series of publications investigated the energy absorption capacity of STF material. Most work reported by Majumdar is on Kevlar fabric and nanosilica-based STF. They studied the influence of process parameters like padding pressure and silica concentration in STF on impact performance of Kevlar-STF soft composite, and reported higher STF concentration improves the impact energy absorption in the Kevlar-STF soft composite. Hasanzadeh et al. (Ref 22) recently published a comprehensive review on rheological properties of STFs with emphasis on stab and ballistic impact applications.

This study follows two aims: first is to assess shear-thickening characteristic of the fumed silica Aerosil OX 50 suspended in polyethylene glycol as a new suspending agent under low- and high-velocity impact loading. Second, this study tries to look into the performance of STF material alone under high shear rate by subjecting the actual STF material to high-velocity impact of a projectile and compare it with neat polyethylene glycol fluid.

2. Materials and Methods

Fumed silica oxide Aerosil OX 50 from Evonic (Germany) was used as a suspending material, Aerosil OX 50 has particle size of 40 nm and BET surface area of 50 m^2/g. Polyethylene glycol (PEG) and ethylene glycol both (EG) with average molecular weight 200 and 62.07 g/mol, respectively, were used as the continuous medium materials. They were obtained from Kimyagaran Emrooz chemical industries co (Iran). The selections were due to their low volatility and thermal stability. Two types of fabric were used for ballistic tests, i.e., Twaron® CT706 woven roving fabric and T 717 woven filament-yarn-based from Tejin Aramid (Amhem/Netherland). Twaron T 717 is a plain filament-yarn-based and Twaron® CT706 woven roving fabrics comprising poly-paraphenylene terephthalamide (PPTA); according to the manufacture, both fabrics are for ballistic applications. The specifications for Twaron T717 and CT706 are given in Table 1 (Ref 23). In order to assess low-velocity impact of STF, open cell polyurethane flexible foam (15 × 10 × 2 cm) with a density of 8.5 kg/m^3 was soaked in the STF suspension containing different amounts of fumed silica.

2.1 Shear-Thickening Fluid Preparation

STF was prepared by dispersion of 20, 30, and 40 wt.% Aerosil OX 50 fumed silica particles in polyethylene glycol (PEG) using ultra-sonication (Bandelin HD3200 Germany, with probe 76-KE and 70 kwatt power) and shear mixing methods at 8000 RPM. Through a combination of a high-speed homogenizer at 8000 RPM and sonication, the particles were dispersed in the polyethylene glycol. Ethanol was used to decrease the surface tension of the dispersion to enable better dispersion of fumed silica particles at 40 wt.% loading in the PEG. Ethanol was later removed via the evaporation process at 80 °C. Ethylene glycol was also used as an alternative continuous medium. A similar method was adopted to introduce the fumed silica particles in the ethylene glycol. Loading concentrations of silica particles in the ethylene glycol were also at 20, 30, and 40 wt.%.

2.2 Rheology Test

Aerosil OX 50 suspensions were characterized using an Anton Paar MCR300 stress-controlled rheometer with a torque range from 0.5 μN m to 120 mN m with a torque resolution of 0.002 μN m. Frequencies range used were from 0.001 to 100 Hz, and the shear rate was 0 to 1000 s^{-1}.

2.3 Impregnation of Twaron Fabric Targets with STF

The impregnation of the target was carried out by soaking the fabric specimen (150 × 250 mm) for 30 min in the STF containing bath with the required particle concentration and then passed through two steel rollers to squeeze out excess STF. In the case of multiple ply systems, each ply was soaked in the STF before being placed together. In order to help impregnation of the fabrics in the case of high particle loading (40 wt.%), the controlled amount of ethanol was added to the STF and removed after impregnation by evaporation. The areal densities of the impregnated fabric targets were determined by weighing the different fabric ply systems before and after impregnation with STF (see Table 1). The target specimens were prepared in 2, 4, and 6 layers.

2.4 Impregnation of Flexible Foam with STF

In order to assess the energy absorption of the STF material as a padding device, open cell polyurethane flexible foam with the density of 8.5 kg/m^3 was saturated in the selected STF

material containing 40 wt.% of fumed silica particles via slow suction of fluid by uncompressing immersed flexible foam samples inside STF containing bath.

2.5 Low-Velocity Drop Weight Impact Test

Low-velocity free fall drop weight impact test was carried out per ASTM D1709 on STF saturated polyurethane flexible foam (120 × 100 × 10 mm) containing 40 wt.% OX 50 fumed silica particles. The test consists of a free fall drop weight device using modified Daventest device from Davenport Ltd (UK) and witness clay pad, and the latter was used to measure the amount of indentation mark. Figure 1 shows a schematic representation of low-velocity drop weight impact test-up. The drop weight test was carried out from 1 m height using 550 and 200 g weight including holder. The indentation mark on the witness clay was measured by casting unsaturated polyester resin in the indented area and measuring the height of the cast resin as a measure for the indentation depth. Three tests were carried out for each weight on different samples, and the average indentation mark is reported here

2.6 Ballistic Impact Test

High-velocity impact tests were carried out using a gas gun (Fig. 2). The gas gun consists of 1.75 m-long smooth barrel with an inside diameter of 8.7 mm, a fast acting high pressure release valve, a breech unit, a supply gas vessel, a 500 ml gas reservoir for each shot release, a target holder, two velocity measuring units, and ballistic paste to catch the projectile intact.

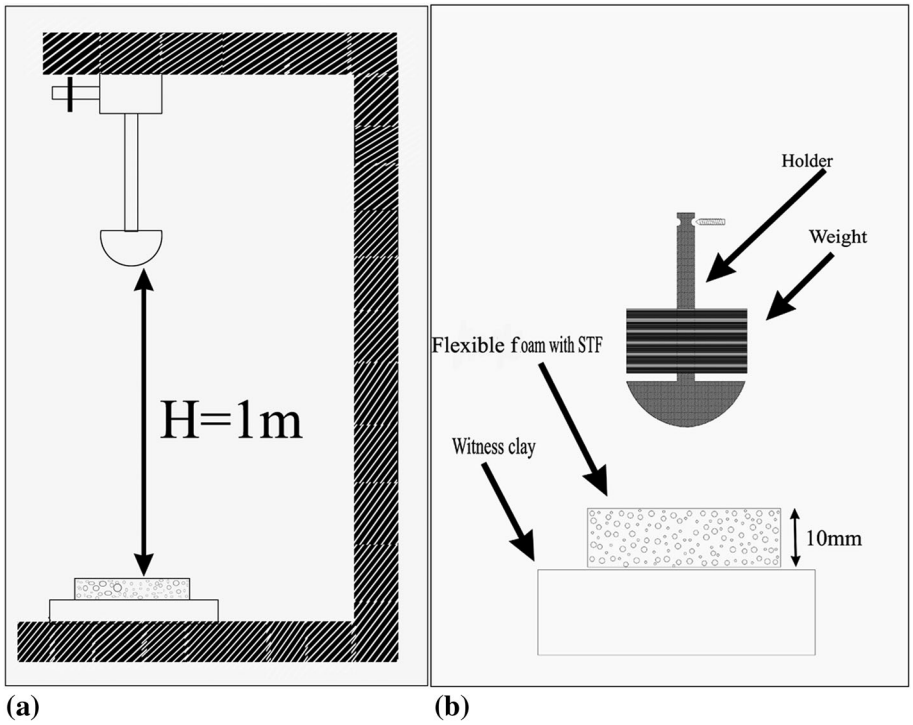

Fig. 1 (A) Schematic representation for low-velocity drop weight impact test-up, (B) Weight, flexible foam with STF and witness clay details

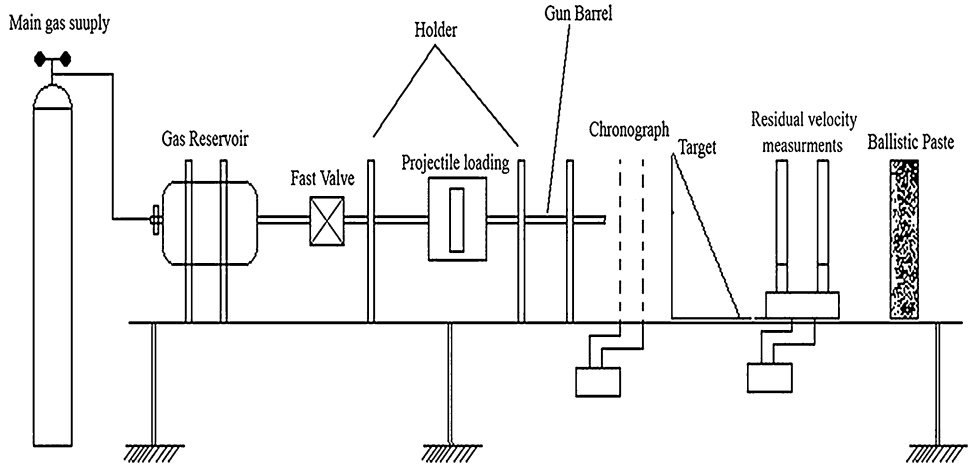

Fig. 2 High-velocity impact test device

The initial velocity of projectile was measured after it was propelled from the gun barrel using a chronograph F-1 model from Shooting Chrony Co Canada. Due to unpredictable line of flight of the projectile after exiting the target, the residual velocity of the projectile which perforated the specimen was recorded using two sets of wide screen aluminum foil panels connected in series via a 1 GHz fast counter. The 15×25 cm specimen was clamped at all four edges. Ballistic limit velocities were determined using (MIL-STD-662F standard). The tests were carried out in a velocity range of 50 to 220 m/s. The projectile used for all high-velocity impact tests was a hemispherical tip hardened steel (Rc60) of 26.5 mm total length, 8.7 mm diameter, and 11.54-g weight. Ballistic tests were carried out on dry 2-, 4-, and 6-layered Twaron fabric and corresponding 40 wt.% STF containing pre-impregnated same fabric in a velocity range of 50 to 220 m/s. Three tests were carried out for each velocity, and average is reported here.

2.7 High-Velocity Impact Test on Neat STF Material

In order to assess the neat STF material (without aramid fabrics) under high-velocity impact, neat STF material containing different amounts of fumed silica particles was subjected to high-velocity impact test. The neat STF was placed in an $8 \times 5 \times 2$ cm thin polyethylene film bag with 15 μm thickness and then heat sealed. The polyethylene bag containing neat STF was then placed in a special fixture. The schematic setup for the neat STF high-velocity impact test is shown in Fig. 3. The test was conducted in three velocity range, i.e., 78, 112, and 143 m/s. Three tests were carried out for each velocity, and average is reported here. The results for the high-velocity impact test on the neat STF material are presented in Table 2. The number in the right-hand side of the first column in Table 2 represents the silica percentage in the STF material used.

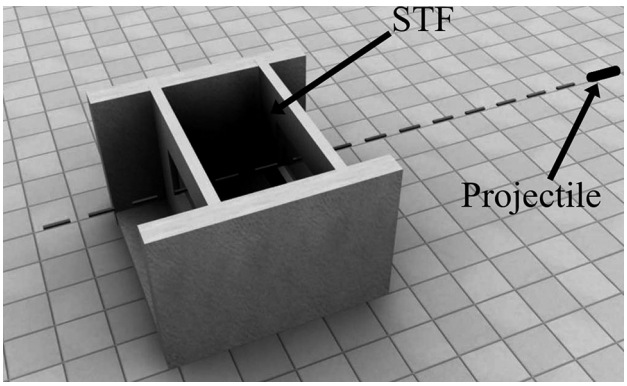

Fig. 3 Schematic setup for the neat STF high-velocity impact test

3. Results and Discussion

3.1 Rheological Study

Rheological assessments were made for STF containing the two types of continuous medium, i.e., polyethylene glycol and ethylene glycol. Viscosity versus shear rate for each material is depicted in Fig. 4 and 5. Both figures present three distinct regions, a relative shear thinning at low shear rate for all three compositions, i.e., 20, 30, and 40 wt.% silica containing, and at

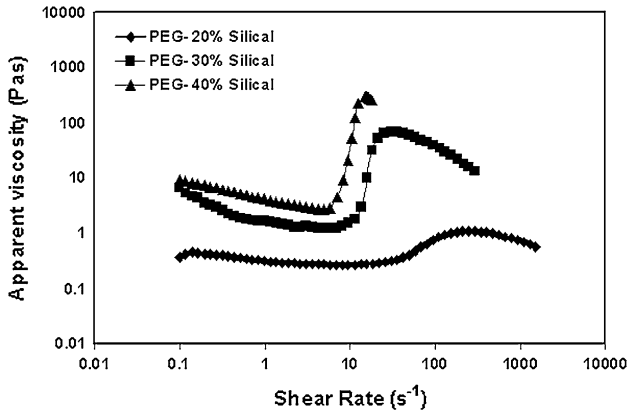

Fig. 4 Apparent viscosities versus Shear rate for the STF with polyethylene glycol

Table 2 Results for high-velocity impact tests on neat STF containing 0, 30 and 40 wt.% silica

Specimens code	STF containing fumed silica particles, wt.%	Initial Impact velocity, m/s	Projectile residual velocity, m/s	Energy absorbed by the target, J
1-PEG40	40	78.5 (1.2)	58.3 (2.4)	15.97
2-PEG40	40	112.3 (1.3)	98.9 (2.1)	16.39
3-PEG40	40	143.2 (1.8)	131.8 (2.6)	18.02
1-PEG40(a)	40	39 (1.1)	26 (1.6)	4.88
2-PEG 40(a)	40	88 (1.3)	79 (1.9)	8.68
3-PEG 40(a)	40	167 (2.1)	162 (3.4)	9.51
1-PEG30	30	78.5 (0.9)	67.4 (1.4)	9.35
2-PEG30	30	112.3 (1.2)	104.1 (2.2)	10.30
3-PEG30	30	143.2 (1.7)	135.8 (2.3)	11.96
1-PEG0	0	78.5 (1.3)	73.1 (1.9)	4.78
2-PEG0	0	112.3 (1.9)	108.0 (2.8)	5.53
3-PEG0	0	143.2 (1.6)	139.2 (2.6)	6.58

The number on the right-hand side of first column (specimen code) represents percentage of silica in the STF
Numbers in the bracket in the third and fourth columns represents standard deviation on the average of three tests conducted
(a) High-velocity impact on neat STF containing 40% silica using sharp tip projectile

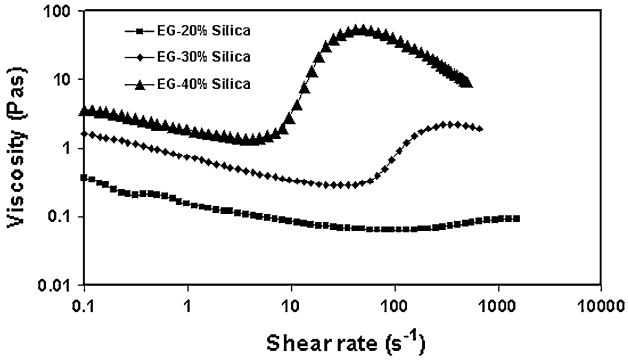

Fig. 5 Apparent viscosities versus Shear rate for the STF with ethylene glycol

high shear rate, the fluid experiences a sudden transition with an increase in viscosity, which signifies shear-thickening behavior and finally a shear thinning like behavior. This shear-thickening characteristic is believed to be due to microstructural changes, i.e., hydrodynamic forces overcome interparticle forces to create particle clusters. When dispersed solid particles in the continuous medium are in contact and hydro cluster phenomenon formed this result in transient fluctuations of particles. This ensues frictions between particles and leads to increase in fluid viscosity; similar anology has been proposed by Brown et al. (Ref 24). Result shows shear-thickening behavior for both 30 and 40 wt.% containing fumed silica in polyethylene glycol medium at a shear rate of about 10 to 100 s^{-1}. The data were collected on a controlled stress rheometer where shear stress was applied, and corresponding shear rates were measured. Rheometery result for 30 wt.% particle containing suspension showed onset of shear thickening at a moderately higher shear rate than 40 wt.% containing suspension. The 20 wt.% containing STF showed very low shear-thickening behavior (see Fig. 4). Other events observed in the viscosity versus shear rate curves for both compositions are the secondary shear thinning like behavior at high shear rate after shear thickening which may be due to plate wall slip. This behavior is an artifact of wall slip, i.e., continuous increase in shear rate results in the STF jamming and thereby STF breakage and plate separation. The result of the ethylene glycol suspension (Fig. 5) shows shear thinning behavior for the 20 wt.% fumed silica containing suspension throughout shear rate tested. The same figure shows moderate shear-thickening behavior commencing between 20 and 50 s^{-1} for 40 wt.% fumed silica containing suspension and between 80 and 500 s^{-1} shear rates for the 30 wt.% containing suspension. Both figures also show shear thinning occurring after shear thickening with an increase in shear rate which again may be attributed to plate wall slip.

3.2 Ballistic Test Results

Considering relative low shear-thickening performance by ethylene glycol based STF and also poor display of shear-thickening by 20 and 30 wt.% fumed silica containing STF in polyethylene glycol (PEG). It was decided to use STF containing polyethylene glycol (PEG) with 40 wt.% fumed silica for the ballistic performance assessment of Twaron fabric impregnated system. High-velocity impact test was conducted on dry 2-, 4-, and 6-layered Twaron fabric and pre-impregnated with STF containing 40 wt.% fumed silica in polyethylene

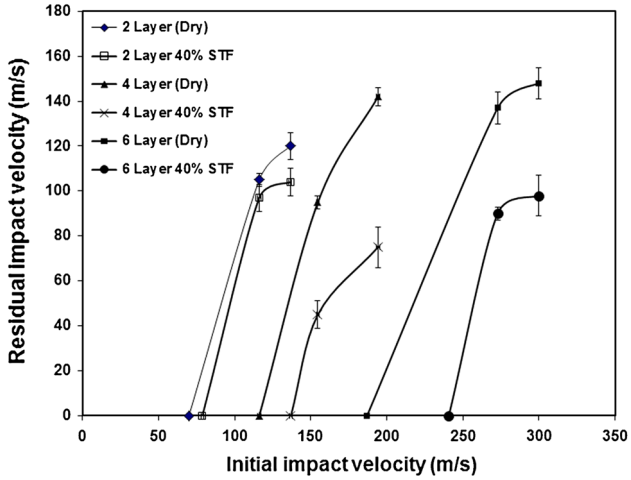

Fig. 6 Impact residual velocities versus impact initial velocity for specimens containing Twaron T717 fabric (Error bars represent standard deviation from the mean value on residual velocity only)

glycol medium. The tests were conducted such that the impact velocity for each set was identical by controlling the gas pressure in the gas gun.

Projectile residual velocity versus impact initial velocity for the Twaron fabrics (T717) tested is depicted in Fig. 6. The figure shows moderate enhancement in ballistic performance in term of lower residual velocity for the 4- and 6-layered STF impregnated specimens compared to corresponding dry Twaron fabric, i.e., STF impregnated fabrics showing better penetration resistance compared to dry fabrics. This better performance though not very significant can be attributed to the higher number of fibers remaining in contact with the projectile surface area during penetration and perforation of the STF impregnated fabric. The higher number of fibers in contact with the projectile surface area can be directly related to friction enhancement associated with the STF coat on the fabric, i.e., avoiding fiber slippage, similar reasoning on the issue of friction has also been reported by other researchers (Ref 6, 7). This consequently results in a higher number of fiber fractures as depicted in Fig. 7(A). Close result between the dry and STF-coated fabric in the 2-layered specimens may be due to limited surface contact between the STF impregnated fabric and the projectile surface area. Comparison of ballistic limit velocities (impact velocity with zero residual exit velocity) confirms that as the number of layers increases, STF plays a better role (see Fig. 8). The figure shows that the highest ballistic limit velocity is associated with 6-layered aramid (T 717) with 40% silica containing STF materials. Ballistic performance for the Twaron plain woven roving (CT 706) with a lower areal density was also investigated. Projectile's residual velocity versus impact velocity for the dry and 40 wt.% fumed silica containing SFT pre-impregnated fabric (CT 706) are presented in Fig. 9. The result shows rather weak performance of the fabric; this low performance in two- and four-layered specimens tested may be attributed to wedge through phenomena, i.e., loose weave density of the fabric results in pushing aside the fibers directly in contact with the projectile allowing the projectile to go through the fabric without getting engaged with the primary fibers. This is directly related to fabric density and weave architecture; similar observation on the significance of fabric weave density on ballistic performance is reported by Chee-

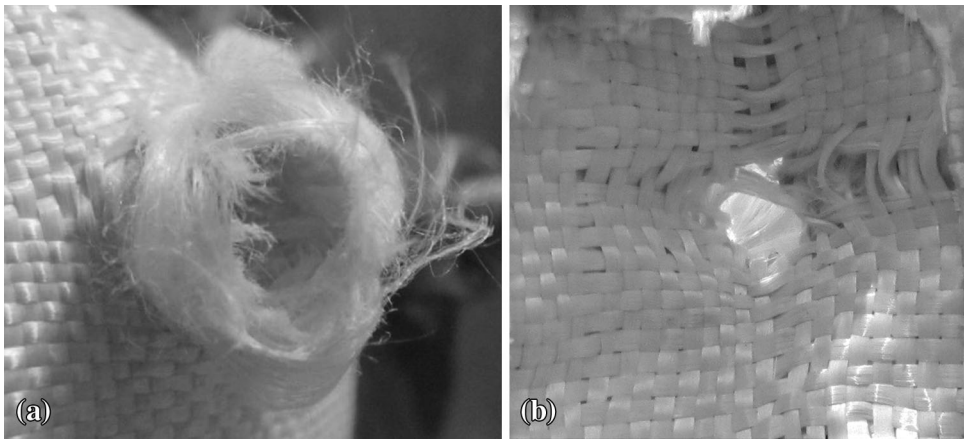

Fig. 7 (A) fiber fracture extension in Twaron 717 woven filament-yarn-based fabrics, (B) shows wedge through phenomena in Twaron CT 706 woven roving

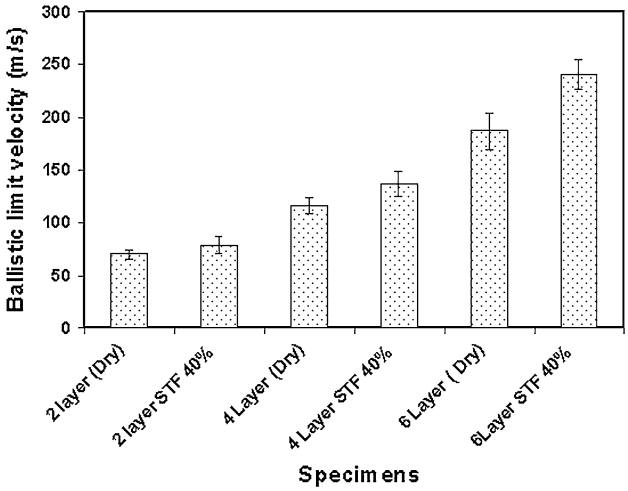

Fig. 8 Ballistic limit velocities for each specimen, (fabric used Twaron T717)

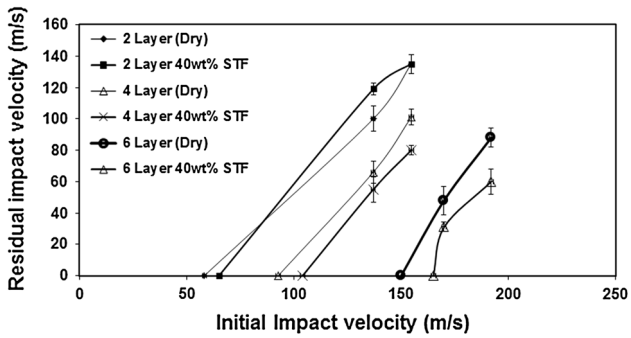

Fig. 9 Impact residual velocities versus impact initial velocity for specimens containing Twaron CT 706 plain woven roving (Error bars represent standard deviation from the mean value on residual velocity only)

seman (Ref 5). The loose weave density of Twaron CT 706 results in projectile slip through the opening (see Fig. 7B). Ballistic limit velocity assessment for the loose fabric (CT706) revealed the weak performance of the fabric for both pre-impregnated with STF material and dry. This is depicted in Fig. 10. The figure indicated that, despite higher ballistic limit velocity for STF-coated fabric compared to a dry one, which is an indicative of some contribution from STF, the values obtained were much lower than corresponding values for Twaron T717 fabric type. Figure 11 presents the energy absorption at ballistic limit velocity for both types of reinforcements (Twaron T 717 and CT706). The figure shows increase in energy absorption with increase in number of layers for both types of reinforcement used. Further study of the figure reveals better energy absorption by the specimens with STF materials having 40% silica than corresponding dry fabric; this is regardless of the number of layers in the specimen. Also, the figure emphases and confirms as in Fig. 6 the significance of better performance in the thicker specimens with STF material, i.e., 6 layered. Comparison of the two fabrics clearly shows that the aramid woven fabric (Twaron T 717) outperforms the

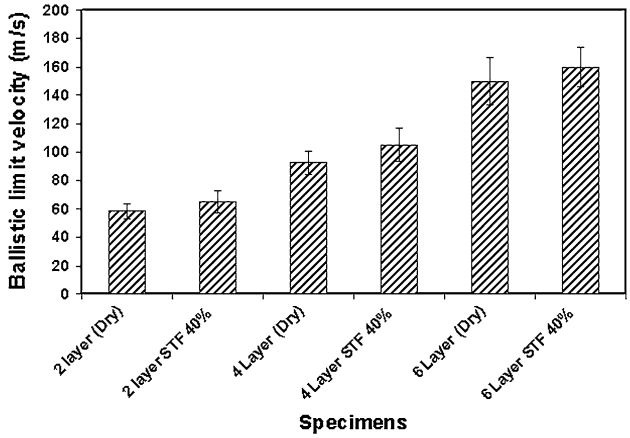

Fig. 10 Ballistic limit velocities for each specimen, (fabric used Twaron plain CT 706)

woven roving type (Twaron CT 706) in term of energy absorption. In order to study the effect of the added weight due to 40 wt.% silica containing STF, the normalized energy absorption for each specimen was calculated using fabric weight (given Table 1) and Equation 1.

$$\text{Normalized energy absorption} = \left(\tfrac{1}{2}mv^2\right)/\text{weight of reinforcement} \quad \text{(Eq 1)}$$

where m is the mass, and v is the projectile velocity.

Figure 12 presents the normalized energy absorption of the high-velocity impact on multi-layered dry and STF containing Twaron fabrics. The figure, however, shows reduced performance when the energy absorptions are normalized to fabric weight. This reduced performance is more pronounced in two- and four-layered specimen containing STF. This again emphasizes the importance of higher surface area and the frictional role played by the thicker specimen, i.e., 6 layer. Generally, comparison of the high-velocity impact results for the STF-coated fabric specimens to that of similar results by others researchers were rather difficult, as each report adopted different methods of assessment of the ballistic performance. However, most reports indicated confliction on the performance in that some reported considerably better ballistic performance by the SFT-coated aramid fabrics compared to our findings (Ref 11, 25), and some others reported similar level of performance (Ref 26, 27). This confliction in the ballistic performance can be attributed to a number of reasons, namely nano-silica used by the other researchers in the preparation of the STF was in order of 300 to 450 nm as against 50 nm used in our report. Specimen size as well as the boundary conditions for the ballistic tests also has a significant effect on the ballistic performance.

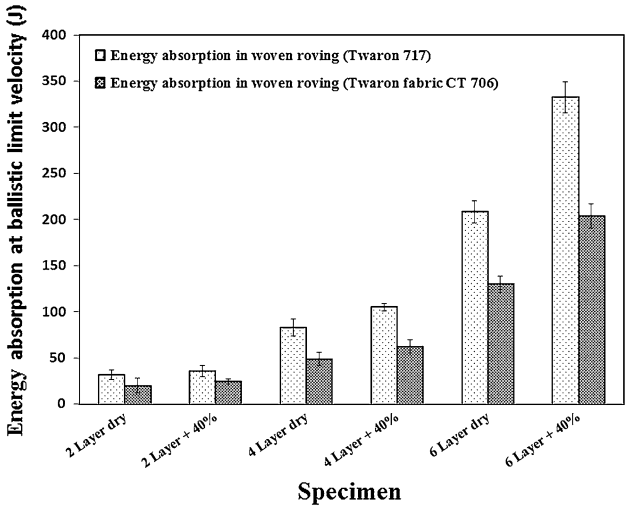

Fig. 11 Energy absorption performance for different dry and STF impregnated aramid fabrics

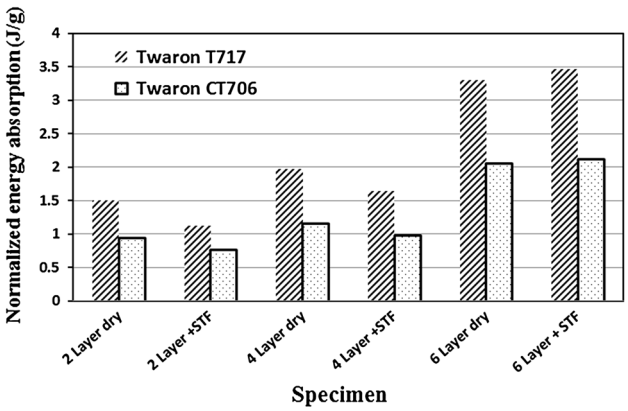

Fig. 12 Normalized energy absorption for different dry and STF impregnated aramid fabrics

3.3 Neat STF Ballistic Test Results

In order to assess STF performance toward high-velocity impact, ballistic tests were also carried out on neat STF itself containing 30 and 40 wt.% fumed silica (Arosil OX50) as well as neat PEG with no silica particles which is designated as STF with 0 wt.%. The test was carried out on a special fixture encapsulating STF material in a thin-walled polyethylene film (see Fig. 3 for the setup). Projectile used was similar to the one used in the ballistic tests done on STF impregnated Twaron fabrics. Table 2 presents impact test results for the neat STF at high-velocity loading. The performance of neat STF toward various impact velocities is also presented graphically in Fig. 13. The study of the figure and energy absorption shown in Table 2 reveals that the high-velocity impact of a hemispherical tip projectile on the neat STF containing 40 wt.% silica performs relatively better at a lower impact velocity compared to STF with 30 wt.% silica for the same projectile impact; this may be directly attributed to an earlier transition to higher viscosity in the neat STF containing 40 wt.% silica under shear rate (see Fig. 4); this signifies earlier shear-thickening behavior. Further assessment of the results in Table 2 showed that with an increase in impact velocity, we witness moderate increase in energy absorption. This was observed practically for all the specimens tested (see Table 2). This behavior may be attributed to the fact that at low velocity, the strain rate associated with the projectile velocity is in the region near the lower part of STF's critical shear rate (see Fig. 4), whereas at two higher impact velocities, the strain rate is well within STF's critical shear rate (the rate at which the shear forces pushing the particles together are equivalent to the repulsive particle interactions) where STF plays its role, i.e., silica particles enter a state of flocculation and are no longer held in suspension. They begin to behave like solids (Ref 24). Figure 14 shows perforated hole just after impact on neat STF. This clearly shows a state of flocculation.

Results revealed that for the hemispherical head projectile, the highest energy absorption is associated with STF with 40% silica followed by STF containing 30% silica.

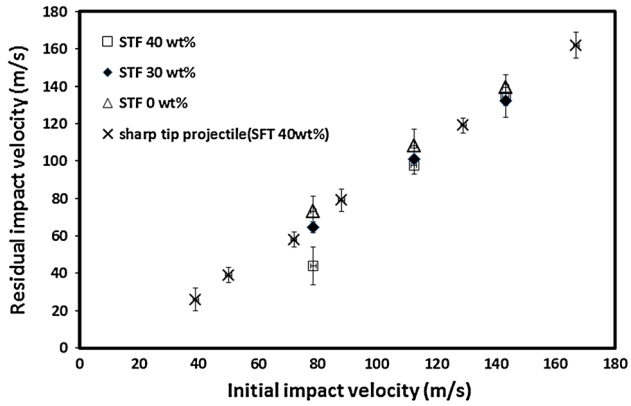

Fig. 13 Residual impact velocities versus Impact initial velocity for neat STF (Error bars represent standard deviation from the mean value on residual velocity only)

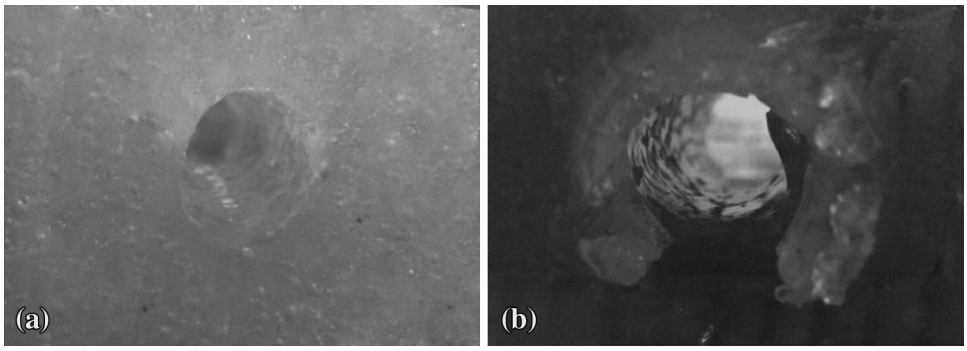

Fig. 14 (A) Neat STF hardens (fluid-solid transition) in the perforated hole, (B) fluid-solid transition reversing seconds after perforation

Table 3 Low-velocity impact test result on flexible foam

Specimens code	Witness clay indentation for 550 g Weight, mm	Witness clay indentation for 200 g Weight, mm
Neat witness clay	24.8 (0.2)	15.3 (0.1)
Neat foam (1 layer)	20.7 (0.4)	12.4 (0.1)
Foam + Polyethylene glycol	20.2 (0.7)	12.1 (0.8)
Foam + Polyethylene glycol + STF 40 wt.%	11.1 (0.7)	6.1 (0.9)

Numbers in the bracket represents standard deviation from average of three measurements

The neat STF was also tested to assess its performance toward different projectile tips under high-velocity impact. Sharp tip conical projectile (15° half angle) was used for this test and compared with a hemispherical tip hardened steel projectile. The neat STF with 40 wt.% fumed silica was selected for the sharp tip projectile high-velocity impact test. The results for this test are also presented graphically in Fig. 13 and Table 2. The study of energy absorption for the two projectiles tested revealed moderately better performance by the hemispherical head projectile. The energy absorption results for the sharp tip conical projectile impact are almost comparable to specimen with no silica particles (see Table 2).

3.4 Low-Velocity Drop Weight Impact Test Results

Results for low-velocity drop weight impact test on a flexible foam (120 × 100 × 10 mm) soaked with the STF are presented in Table 3. In this test, indentation from free fall drop weight of 550 and 220 g is investigated. The cases considered include measured indentation by free fall drop weight on neat witness clay, flexible foam placed on the witness clay, flexible foam soaked in polyethylene glycol, and flexible foam soaked in STF containing 40 wt.% silica particles. The result shows approximately 50.8% reduction in indentation mark on the witness clay for the flexible foam soaked in STF containing 40 wt.% silica particles compared to dry flexible foam for the 220 g weight drop and a reduction of 46.4% for the 550 g weight drop. This clearly shows the significance of the STF presence in energy absorption under low-velocity impact (4.5 m/s). Similar comparison of the 220 and 550 g drop weight on the flexible foam soaked in neat polyethylene glycol with that of flexible foam soaked in STF containing 40 wt.% silica particle shows 49.5 and 45% reduction in witness clay indentation mark for the latter case, respectively.

4. Conclusions

The effect of nano-sized fumed silica particles (Areosil OX 50) as the suspending particles in a shear thickened fluid (STF) and its response to various impact loads were investigated. Three areas were studied, namely ballistic performance of STF pre-impregnated aramid fabric, neat STF under high-velocity impact, and low-velocity drop weight impact on a flexible foam soaked in STF. Following conclusion can be drawn from the result obtain.

- Polyethylene glycol as the continuous medium showed better shear-thickening behavior compared to ethylene glycol.
- Maximum shear thickening occurred at 40 wt.% fumed silica particles.
- STF pre-impregnated aramid fabrics showed moderate energy absorption in only thick section specimens (multi-layered).
- Friction was postulated to be the main mechanism in pre-impregnated aramid fabrics energy absorption.
- Fabric architecture and areal density also played important role in energy absorption, with loose fabric showing little effect of STF incorporation.
- Neat STF showed good energy absorption at velocities near STF's critical shear rate.
- Flexible foam-filled STF showed good energy absorption revealing its potentials as impact protection padding material.

References

1. H.A. Barnes, Shear-Thickening (dilatancy) in Suspensions of Non-Aggregating Solid Particles Dispersed in Newtonian Liquids, *J. Rheol.*, 1989, **33**(2), p 29–357
2. A.J. Liu and S.R. Nagel, Nonlinear Dynamics—Jamming is Not Just Cool Anymore, *Nature*, 1998, **396**(21), p 21–26

3. J.W. Bender and N.J. Wagner, Reversible Shear Thickening in Monodisperse and Bi-disperse Colloidal Dispersions, *J. Rheol.*, 1996, **40**(5), p 899–916
4. F. Cunniff, An Analysis of The System Effects in Woven Fabrics Under Ballistic Impact, *Text. Res. J.*, 1992, **62**(9), p 495–509
5. B.A. Cheeseman and T.A. Bogetti, Ballistic Impact into Fabric and Compliant Composite Laminates, *Compos. Struct.*, 2003, **61**(1-2), p 161–173
6. B.J. Brisco and F. Motamedi, The Ballistic Impact Characteristics of Aramid Fabrics: The Influence of Interface Friction, *Wear*, 1992, **158**(1-2), p 229–247
7. B.J. Brisco and F. Motamedi, Role of Interfacial Friction and Lubrication in Yarn and Fabric Mechanics, *Text. Res. J.*, 1990, **60**(12), p 697–703
8. L. Lavielle, Polymer-Polymer Friction: Relation to Adhesion, *Wear*, 1991, **151**(1), p 63–75
9. B.L. Lee and T.F. Walsh, Penetration Failure Mechanisms of Armor-Grade Fiber Composites Under Impact, *J. Compos. Mater.*, 2001, **35**(18), p 1605–1633
10. A.R. Sabet, M.H. Beheshty, and H. Rahimi, High Velocity Impact Behavior of GRP Panels Containing Coarse-Sized Sand Filler, *Polym. Compos.*, 2008, **29**(8), p 932–939
11. Y. Lee, E.D. Wetzel, and N.J. Wagner, The Ballistic Impact Characteristics of Kevlar® Woven Fabrics Impregnated with a Colloidal Shear Thickening Fluid, *J. Mater. Sci.*, 2003, **38**(13), p 2825–2833
12. M.J. Decker, C.J. Halbach, C.H. Nam Laufer, and N.J. Wagner, Stab Resistance of Shear Thickening fluid (STF)-Treated Fabrics, *Compos. Sci. Technol.*, 2007, **67**(3-4), p 565–578
13. N.J. Wagner and A. Brady, Shear Thickening in Colloidal Dispersions, *Phys. Today*, 2009, **62**(10), p 27–32
14. B.A. Rose, C.H. Nam Laufer, D.P. Kalman, E.D. Wetzel, and N.J. Wagner, Multi-Threat Performance of Kaolin-Based Shear Thickening Fluid (STF)-Treated Fabrics. *Proceedings of SAMPE*, June 3-7, 2007 (Baltimore, MD), 2007
15. A.S. Lim, S. Lopatnikov, N.J. Wagner, and J.W. Gillespie, Investigating The Transient Response of a Shear Thickening Fluid Using The Split Hopkinson Pressure Bar Technique, *Rheol. Acta*, 2010, **49**(8), p 879–890
16. J.A. Hassan, V.K. Rangari, and S. Jeelani, Synthesis, Processing and Characterization of Shear Thickening Fluid (STF) Impregnated Fabric Composites, *Mat. Sci. Eng. A*, 2010, **527**(12), p 2892–2899
17. B.W. Lee and C.G. Kim, Computational Analysis of Shear Thickening Fluid Impregnated Fabrics Subjected to Ballistic Impacts, *Adv. Compos. Mater.*, 2012, **21**(2), p 177–192
18. A. Srivastava, A. Majumdar, and B.S. Butola, Improving the Impact Resistance of Textile Structures by Using Shear Thickening Fluids: A Review, *Crit. Rev. Solid State*, 2012, **37**(2), p 115–129
19. A. Majumdar, B.S. Butola, and A. Srivastava, Optimal Designing of Soft Body Armour Materials Using Shear Thickening Fluid, *Mater. Des.*, 2013, **46**, p 191–198
20. A. Majumdar, B.S. Butola, and A. Srivastava, An Analysis of Deformation and Energy Absorption Modes of Shear Thickening Fluid Treated Kevlar Fabrics as Soft Body Armour Materials, *Mater. Des.*, 2013, **51**, p 148–153
21. A. Majumdar, B.S. Butola, and A. Srivastava, Development of Soft Composite Materials with Improved Impact Resistance Using Kevlar Fabric and Nano-Silica Based Shear Thickening Fluid, *Mater. Des.*, 2014, **54**, p 295–300
22. M. Hasanzadeh and V. Mottaghitalab, The Role of Shear-Thickening Fluids (STFs) in Ballistic and Stab-Resistance Improvement of Flexible Armor, *J. Mater. Eng. Perform.*, 2014, **23**(4), p 1024–1544
23. Ballistic Material Handbook, Teijin Company, http://www.teijinaramid.com/wp-content/uploads/2013/05/Teijin-Aramid-Ballistics-Material-Handbook-English1.pdf. Accessed May 2014
24. E. Brown, H. Zhang, N.A. Forman, B.W. Maynor, D.E. Betts, J.M. Desimone, and H.M. Jaeger, Shear Thickening and Jamming in Densely Packed Suspensions of Different Particle Shapes, *Phys. Rev. E*, 2011, **84**(3), p 031408
25. P.J. Lyoul, B. Yoon, J.G. Paik, and T.J. Kang, Ballistic Performance of p-Aramid Fabrics Impregnated with Shear Thickening Fluid; Part I—Effect of Laminating Sequence, *Text. Res. J.*, 2012, **82**(6), p 527–541
26. V.B.C. Tan, T.E. Tay, and W.K. Teo, Strengthening Fabric Armour with Silica Colloidal Suspensions, *Int. J. Solids Struct.*, 2005, **42**(5), p 1561–1576
27. E.V. Lomakin, P.A. Mossakovsky, A.M. Bragov, A.K. Lomunov, A.Y. Konstantinov, M.E. Kolotnikov, and M.S. Vakshtein, Investigation of Impact Resistance of Multilayered Woven Composite Barrier Impregnated with the Shear Thickening Fluid, *Arch. Appl. Mech.*, 2011, **81**(12), p 2007–2020